FULL PAPER

Improving the Conversion and Energy Efficiency of Carbon Dioxide Splitting in a Zirconia-Packed Dielectric Barrier Discharge Reactor

Koen Van Laer* and Annemie Bogaerts[a]

The use of plasma technology for CO_2 splitting is gaining increasing interest, but one of the major obstacles to date for industrial implementation is the considerable energy cost. We demonstrate that the introduction of a packing of dielectric zirconia (ZrO_2) beads into a dielectric barrier discharge (DBD) plasma reactor can enhance the CO_2 conversion and energy efficiency up to a factor 1.9 and 2.2, respectively, compared to that in a normal (unpacked) DBD reactor. We obtained a maximum conversion of 42% and a maximum energy efficiency of 9.6%. However, it is the ability of the packing to almost double both the conversion and the energy efficiency simultaneously at certain input parameters that makes it very promising. The improved conversion and energy efficiency can be explained by the higher values of the local electric field and electron energy near the contact points of the beads and the lower breakdown voltage, demonstrated by 2D fluid modeling.

Introduction

To mitigate and ultimately stop global warming, the emission of greenhouse gases by human sources must be reduced. As CO_2 is one of the most important greenhouse gases, in recent years, there has been a growing interest in carbon capture and utilization (CCU) technologies.[1–3] The splitting of CO_2 by a plasma is one of these technologies. A plasma is a partially ionized gas that consists of neutral species, ions, electrons, excited species, radicals, and photons. Plasma is very promising for CO_2 splitting because the entire gas does not need to be heated as in classical thermal splitting. Instead, only the electrons are heated by the electric field, which leads to electron impact excitation, ionization, and dissociation reactions. In this way, inert gases such as CO_2 can be split at a reasonable energy cost.

The type of plasma that is exploited for CO_2 splitting most commonly is the dielectric barrier discharge (DBD). In a DBD reactor, the plasma is created by applying an electric potential difference between two electrodes of which at least one is covered by a dielectric material.[4,5] A DBD reactor has several advantages for CO_2 splitting: it operates at atmospheric pressure and it has a simple construction, which can be easily scaled up for industrial applications, as demonstrated in the past for the production of ozone.[5] It can also be switched on and off easily and is, therefore, very promising to be used for the storage of renewable energy during peak moments on the grid.[6] Moreover, it can be combined easily with a catalyst for the selective production of value-added chemicals if CO_2 is mixed with a H-source gas, such as CH_4 or H_2O. However, the energy efficiency of a DBD reactor for CO_2 splitting with a reasonable conversion is still too limited, that is, in the order of 2% for a maximum obtainable conversion of 34%.[7] Likewise, under other conditions (i.e., low power and high gas flow rate), a maximum energy efficiency of 9% can be reached, but the conversion is then only 8%. The improvement of the energy efficiency while a reasonable conversion is maintained is, therefore, the major challenge in research on CO_2 splitting by DBD plasmas.

The most promising way to accomplish this is by introducing a packing of dielectric beads into the DBD reactor. It has been demonstrated already for other applications, such as the destruction of volatile organic compounds (VOC), that a so-called packed-bed DBD reactor yields higher conversions and energy efficiencies.[8–14] In contrast, there are few available papers about CO_2 splitting in a packed-bed DBD reactor,[15,16] especially with regard to energy efficiency. Yu et al. studied the decomposition of CO_2 in a packed-bed DBD reactor using different packing materials, that is, silica gel, quartz, α-Al_2O_3, γ-Al_2O_3, and $CaTiO_3$.[15] The best results were found with a $CaTiO_3$ packing, which boosted the conversion from 12.5 to 20.5%. The energy efficiency is not mentioned in their paper but can be calculated from the reported data to be 4.8% at maximum conversion, which is a factor of 1.7 higher than that without packing. The maximum energy efficiency was 6%, which corresponds to a conversion of only 15.6%. Recently, Mei et al. obtained similar results using glass beads and $BaTiO_3$ as packing materials at different input powers.[16] A 75% increase to a maximum conversion of 28% was reached by introducing a packing of $BaTiO_3$ beads. The energy efficiency was discussed briefly

[a] K. Van Laer, Prof. Dr. A. Bogaerts
    Research group PLASMANT, Department of Chemistry
    University of Antwerp
    Universiteitsplein 1
    2610 Wilrijk-Antwerp (Belgium)
    E-mail: koen.vanlaer@uantwerpen.be

and reached a maximum of 0.254 mmol kJ^{-1} (i.e., 7.1 %) for an input power of 20 W and a flow of 50 mL min^{-1}. At this point, the conversion was only 13.8 %.

It has been suggested in the context of VOC remediation[11–13] that the positive effects of a packing are the result of the local enhanced electric field and thus higher electron energies near the contact points of the dielectric beads, which is caused by the polarization of these beads by the external electric field. In other words, the applied electrical energy will be used more efficiently to induce chemical reactions.

As plasma diagnostics in a packed-bed DBD reactor are not straightforward because of limited physical and optical access caused by the packing, a computer model is of particular interest. In the past, only a few numerical studies have been performed for packed-bed DBD reactors.[17–20] Chang et al.[17] and Takaki et al.[18] developed a simplified 1D parallel plate N_2 plasma model that assumed the void between the pellets to be spherical, which of course is not the case in reality. Kang et al.[19] developed a 2D model to study the propagation of a single discharge avalanche from one electrode to the other. The arrangement of the packing beads was limited to either a single bead or two beads on top of each other. However, the study did not include any plasma chemical reactions. Finally, Russ et al.[20] developed a 2D hydrodynamic model that included plasma chemical reactions (for dry exhaust gas, 80 % N_2, 20 % O_2, and 500 ppm NO). However, yet again it only simulated a short one-directional discharge with a constant applied potential.

In this study, we demonstrate an improved conversion and energy efficiency for CO_2 splitting through the introduction of a ZrO_2 packing into the DBD reactor. Although Yu et al.[15] and Mei et al.[16] only used one bead size, we show that a variation of the bead size can have a significant effect on the results. Indeed, by studying the effect of the packing bead diameter together with the input power and gas flow rate, we are able to optimize the discharge towards the highest conversion and highest energy efficiency ever reached to date. Interestingly, we can obtain a high conversion and energy efficiency simultaneously. We were able to gain an insight into the mechanism of the plasma discharge by quantitative computer modeling to help to explain the experimental results.

Results and Discussion

In this section we will discuss the experimental results of the influence of the bead size, flow rate, and applied power on the CO_2 conversion and energy efficiency to help to explain the improvements with our modeling results. We also investigated the effect of these parameters on the selectivities towards the formation of the end products, namely, CO and O_2. However, these selectivities were always around 50 % under all conditions. This is expected as the overall reaction of the splitting process is very simple: $CO_2 \rightarrow CO + 0.5 O_2$. Some traces of O_3 can be formed, but this could not be detected in our GC analysis.

In principle, CO_2 can be absorbed by the ZrO_2 beads, which might be dependent on the particle size. However, we flushed the reactor after opening for at least 20 min with pure CO_2 to make sure no residual air is present. Moreover, we ignited the plasma 20 min before our GC measurements to ensure that the plasma reactor is in steady state when the gas is analyzed. The fact that ZrO_2 can adsorb CO_2 (and CO) will, therefore, not have any influence on the presented results because the ZrO_2 beads will be saturated at the time of measurement. Furthermore, after the plasma treatment, no carbon deposition was found on the reactor walls or the ZrO_2 beads.

Effect of bead size, flow rate, and applied power on CO_2 conversion and energy efficiency

The CO_2 conversion (left) and energy efficiency (right) as a function of bead size for three different gas flow rates and three different applied powers are illustrated in Figure 1. The dotted lines represent the results of the unpacked reactor. It is clear that both the conversion and energy efficiency are influenced strongly by the introduction of a packing in the DBD reactor. Typically, at 60 and 80 W, a larger packing has a strong enhancing effect, whereas a smaller packing can actually decrease the conversion and energy efficiency. The explanation for this phenomenon is probably that the residence time in the reactor filled with a smaller packing is too low to benefit from the enhancing effects of the presence of a packing. Moreover, in the case of a smaller packing with sizes at least four times smaller than the gap distance, the beneficial
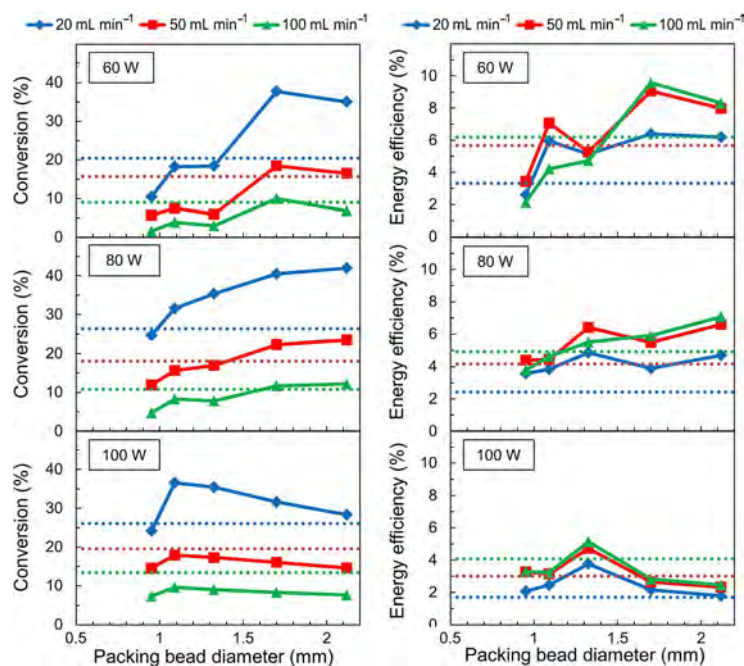

Figure 1. Measured CO_2 conversion (left) and energy efficiency (right) as a function of bead size for three different applied powers and three different gas flow rates. The dotted lines represent the results for the unpacked reactor.

effects of the packing will have to spread over a larger number of contact points, which will make the enhancement at each contact point, and apparently also overall, lower than if fewer contact points are present. Therefore, in the following analysis we focus mainly on the results from the larger bead sizes (1.60–1.80 and 2.00–2.24 mm diameter). Indeed, the highest obtainable conversions and energy efficiencies are reached with these two bead sizes.

Furthermore, it is clear from the results shown in Figure 1 that a lower flow rate will always lead to a higher conversion. This is logical because it corresponds to a longer residence time in the plasma. However, it will lead to a lower energy efficiency, which is shown directly by the equations given in the Experimental Section.

An increase of the applied power will increase the conversion, especially for the smaller bead sizes as the plasma power will also increase. However, if the applied power is above 80 W, the conversion for almost all bead sizes, especially the larger ones, decreases. We believe that this may be attributed to a change in the discharge characteristics, possibly from a more surface type discharge at 80 W to a more filamentary discharge at 100 W, which has been explained in the literature.[21] If this is indeed the case, then we may conclude that the type of discharge that occurs at 80 W is better for CO_2 splitting than that at higher applied power. The energy efficiency, in turn, decreases with increasing applied power, which is again logical from the equations given in the Experimental Section.

Maximum values obtained and comparison with literature

The maximum conversion obtained in this study is 42.0%, which is reached with the largest bead size at the lowest flow rate (20 mL min^{-1}) with 80 W of applied power. The energy efficiency under these conditions is 4.7%. Compared to an empty reactor, the conversion is a factor of 1.6 better and the energy efficiency is almost doubled (i.e., an increase of a factor of 1.9).

The maximum energy efficiency obtained is 9.6%, which is reached with the highest flow rate (100 mL min^{-1}), the lowest applied power (60 W), and bead sizes of 1.6–1.8 mm diameter, but it corresponds to a conversion of only 10.0%. In this case, the improvement of the energy efficiency and conversion over an empty reactor are factors of 1.5 and 1.1, respectively.

The most promising results are obtained for a packing with bead sizes between 1.60–1.80 mm diameter, with an applied power of 60 W, and a flow rate of 20 mL min^{-1}. The conversion at this point reaches 37.8% with a corresponding energy efficiency of 6.4%, which is 1.9 and 1.8 times higher than that without a packing, respectively. This is a very promising result, which shows us that the introduction of a packing can almost double the conversion and energy efficiency simultaneously if the right input parameters are chosen.

The results obtained in this work are compared to the best available results for CO_2 conversion and energy efficiency in
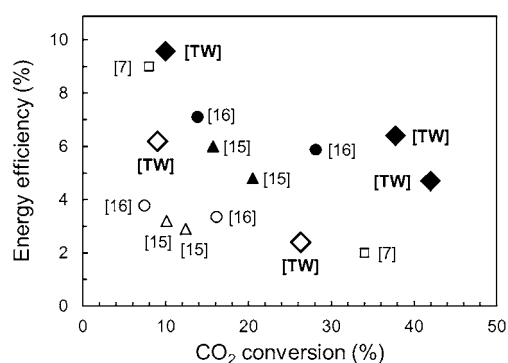

Figure 2. Comparison of CO_2 conversion and energy efficiency values obtained in this work (TW) with best available data in literature for a DBD reactor used for pure CO_2 splitting. The filled points indicate a packed-bed DBD reactor, and the empty points represent the empty reactor.

a (packed-bed) DBD reactor in Figure 2. Notably, the number of papers to compare with is quite limited because there are not so many available for pure CO_2 splitting (i.e., not mixed with a rare gas or CH_4) that mention values for both conversion and energy efficiency. What stands out immediately is that a packed-bed DBD reactor is not only able to generate higher maximum conversions or energy efficiencies but also provides better combined values of conversion and energy efficiency. In other words, the conversion and energy efficiency are both enhanced by the presence of the packing. Furthermore, it is clear that both the maximum obtainable conversion and energy efficiency are further increased in the present work compared to the best available data from literature. This means that a variation of the packing bead diameter, flow rate, and applied power can already lead to better results. In our opinion, the results with combined high conversion and high energy efficiency are the most promising. Indeed, it is not the search for the highest obtainable conversion or the highest possible energy efficiency that should be the focus of future research but the combination of both. We believe that the results can be further improved by studying different packing materials with different dielectric constants in combination with different packing geometries and even the presence of a catalyst on the surface.

Finally, to compare our results with those from the best available technologies, we compared them with studies for pure CO_2 splitting by other types of plasma, that is, microwave plasma and gliding-arc plasma. In the 1970s, Fridman showed that a microwave plasma reactor could be very promising for CO_2 splitting and reported energy efficiencies of 80–90%.[22] However, these results were obtained at reduced pressure (0.02–0.05 bar), which is not practical for industrial implementation. Moreover, working at lower pressure also costs energy, which will decrease the total energy efficiency significantly. To enable a better comparison of our results, we should compare them with results from a microwave plasma at atmospheric pressure. Spencer and Gallimore reported a maximum conversion of 45%, which corresponded to a mere 5% energy efficiency.[23] The maximum energy efficiency of 21% comes with a conversion of 10%. It is

clear that higher energy efficiencies are feasible with a microwave plasma. However, to reach a conversion of at least 25%, the energy efficiency will never exceed 7.5%, which is very similar to our results. An atmospheric-pressure reverse-vortex-flow gliding-arc discharge can reach higher energy efficiencies (18–43%).[24] However, the accompanying conversion is limited to 2–9%. The biggest advantage of microwave and gliding-arc reactors is their ability to cope with very high flow rates that reach 16 and 40 L min^{-1}, respectively. Their biggest disadvantage, however, is that they are not combined as easily with catalysts as a packed-bed DBD reactor. In this respect, we believe that a packed-bed DBD reactor has the biggest advantage towards future improvement and future applications in combination with catalysis for the selective production of value-added compounds.

Insight in the improved conversion and energy efficiency

To better understand the underlying reason for the improved conversion and energy efficiency, we present here the electric field distribution, electron temperature, and electron density, as calculated from our model, for an applied potential of 3.5 kV peak-to-peak at 23.5 kHz.

The presence of a packing in a DBD reactor will enhance the electric displacement field inside the dielectric material strongly near the contact points between the packing beads or between a bead and the dielectric wall and between a bead and the grounded electrode (Figure 3). As a result, the electric field in the gas region will also be stronger near these contact points. Indeed, the applied potential difference between both electrodes causes the dielectric material to polarize. Thus, at the contact points there will be local charges of opposite sign close together, which lead to the locally enhanced electric field. As a result, the electrons will encounter a higher acceleration and thus exhibit a higher electron temperature (Figure 3, middle), which will lead to a breakdown. Moreover, the electron temperature will be higher than that

in an empty DBD reactor for the same applied power, which indicates that the electrons are heated more efficiently to lead to more CO_2 splitting by electron impact dissociation for the same applied power to yield a higher energy efficiency.

The breakdown takes place at the contact point between the two packing beads, which is demonstrated by the high instantaneous electron density of 1.7×10^{17} m^{-3} in this region, plotted 0.5 µs after the moment of breakdown (Figure 3, right). The enhancement of the electric field is indeed stronger here than at the other two contact points. If the applied potential is low, that is, 3.5 kV peak-to-peak or less, the discharge will stay in this region and it will decrease to an electron density of 1.6×10^{13} m^{-3} after 1 µs because of recombination in the plasma and at the walls. However, in the empty reactor model, no discharge was found to take place at this applied potential because it is too low to overcome the breakdown voltage for the entire gas gap. Our model predicts that the empty reactor requires at least 5 kV peak-to-peak to initiate a discharge. Therefore, we can conclude that a packing will lower the breakdown voltage, which is interesting in terms of energy efficiency.

Conclusions

We have demonstrated that a packing of ZrO_2 beads with a diameter of at least 1/3 of the gap size of the dielectric barrier discharge reactor can increase the conversion and energy efficiency of CO_2 splitting significantly. In comparison with an empty reactor, the introduction of a packing can increase the conversion and energy efficiency simultaneously by almost a factor 2. The best combination of conversion and energy efficiency was reached with a bead size in the range of 1.60–1.80 at a flow rate of 20 mL min^{-1} and an input power of 60 W, which yielded values of 37.8% conversion and 6.4% energy efficiency. Our computational results suggest that this increase is caused by the presence of strong electric fields and thus high electron energies at the contact points because of polarization of the packing by the applied potential difference, which thereby lowers the breakdown voltage. The results are very promising and indicate clearly that the introduction of a packing has beneficial effects on the conversion and energy efficiency of CO_2 splitting. We believe that the results can be further improved by searching for the ideal packing geometry and the ideal dielectric constant of the packing material. Finally, a packed-bed dielectric barrier discharge reactor can also be realized with a catalytic packing, which is very promising for the selective conversion of greenhouse gases (CO_2 and CH_4) into value-added chemicals.
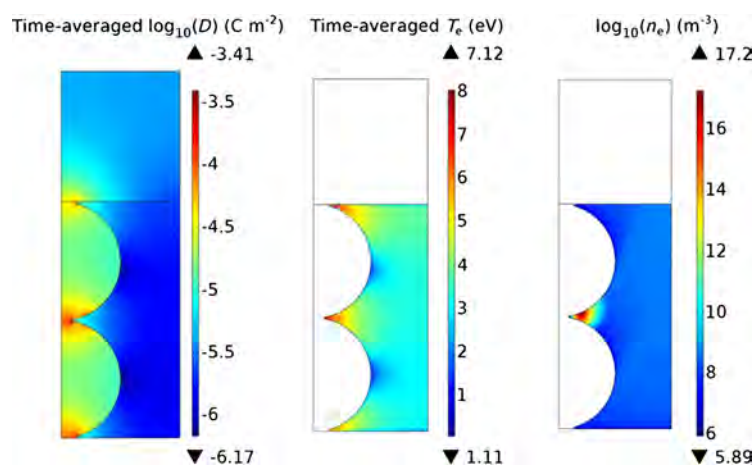

Figure 3. Calculated time-averaged electric displacement field D [C m^{-2}], time-averaged electron temperature T_e [eV], and instantaneous electron density n_e [m^{-3}] (from left to right). The scales on the left and on the right are logarithmic.

Experimental Section

Experimental setup

The experiments were performed by using a cylindrical DBD reactor that consisted of an inner electrode and a coaxial Al_2O_3 tube (Figure 4). The inner electrode was a stainless-steel rod with a diameter of 8.0 mm and was grounded. The Al_2O_3 tube had an inner and outer diameter of 17.0 and 22.0 mm, respectively, and was covered by a nickel foil electrode connected to an AC high-voltage power supply (AFS). It had a length of 90 mm, which defined the length of the discharge. The discharge gap, that is, the distance between inner electrode and Al_2O_3 tube, was fixed at 4.5 mm, which resulted in a discharge volume of 15.9 cm^3. The CO_2 gas flow rate was controlled by using a mass flow controller (EL-flow, Bronkhorst). The total current was recorded by using a Rogowski-type current monitor (Pearson 4100), and a high-voltage probe (Tektronix P6015A) was used to measure the applied voltage. To obtain the charge generated in the discharge, the voltage on the external capacitor was measured. All the electrical signals were sampled by using a four-channel digital oscilloscope (Picotech PicoScope).

Experiments were performed at three different gas flow rates (20, 50, and 100 mL min^{-1}) and three different applied powers (60, 80, and 100 W) with and without ZrO_2 packing. The experiments without packing served as a benchmark to define the improvement in conversion and energy efficiency. The experiments with packing were performed with five different bead size ranges (diameters of 0.90–1.00, 1.00–1.18, 1.25–1.40, 1.60–1.80, and 2.00–2.24 mm) obtained by sieving a mixture of ZrO_2 beads (SiLiBeads). The dielectric constant of the ZrO_2 beads was in the range of 22–25.

To determine the CO_2 conversion and energy efficiency, the CO_2 gas was measured after plasma treatment by using a three-channel compact gas chroma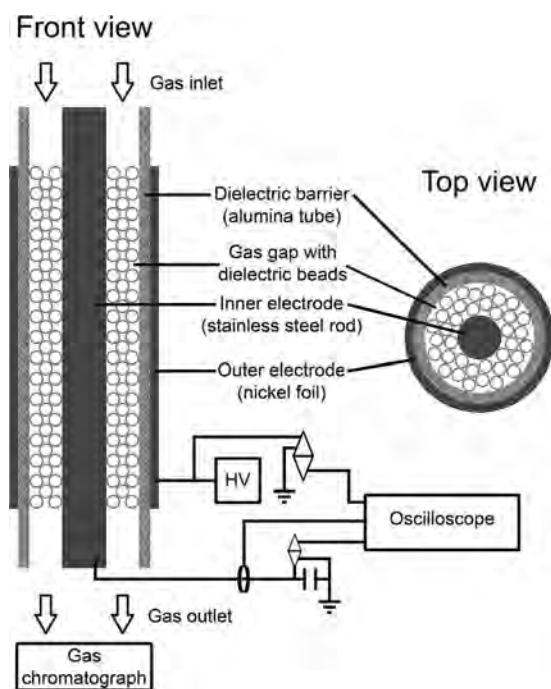tograph (CGC; Interscience) equipped with two thermal conductivity detectors (TCD) and a flame ionization detector (FID). The first TCD channel contained a Molecular Sieve 5A column for the segregation of the molecular gases O_2, N_2, and CO, and the second TCD channel was equipped with an Rt-QBOND column for the measurement of CO_2 and C_1–C_2 hydrocarbons. The FID was equipped with an Rtx-5 column for the measurement of C_1–C_{10}-containing compounds. Benchmark measurements, without plasma treatment, were also performed to measure the CO_2 signal at the inlet. The CO_2 conversion (X_{CO_2}) was then calculated as [Eq. (1)]:

$$X_{CO_2}(\%) = \frac{CO_{2\,inlet} - CO_{2\,outlet}}{CO_{2\,inlet}} * 100\,\%$$ (1)

To calculate the energy efficiency of the process, we first defined the specific energy input (SEI) from the plasma power and the gas flow rate [Eq. (2)]:

$$SEI[kJ\,L^{-1}] = \frac{P_{plasma}[kW]}{Flow[L\,min^{-1}]} * 60\,[s\,min^{-1}]$$ (2)

The plasma power itself is calculated from the instantaneous applied potential $V(t)$ and the measured current $I(t)$ over one period T [Eq. (3)]:

$$P_{plasma} = \frac{1}{T}\int_0^T V(t) * I(t)\,dt$$ (3)

Finally, the energy efficiency is defined as [Eq. (4)]:

$$\eta\,[\%] = \frac{\Delta H_R\,[kJ\,mol^{-1}] * X_{CO_2}\,[\%]}{SEI\,[kJ\,L^{-1}] * molar\,volume\,[L\,mol^{-1}]}$$ (4)

The reaction enthalpy (ΔH_R) is 279.8 kJ mol^{-1} or 2.9 eV molec^{-1}.

Computational details

To gain insight into the influence of a packing on the discharge behavior in a DBD reactor, an axisymmetric 2D fluid model was developed using COMSOL's built-in plasma module.[25] The model was based on solving a set of coupled differential equations that express the conservation of mass, momentum, and energy for the different plasma species. These equations contain production and loss terms for the different species based on the chemical reaction set. For the electrons and positive ions, the flux was based on the drift-diffusion approximation. The Poisson equation was also solved to self-consistently calculate the electric field distribution, and we used the densities of the charged plasma species as input.

Modeling this type of reactor is not straightforward. In principle, the real-life geometry demands a 3D representation in the model. However, to describe the plasma behavior properly an extremely fine mesh is required. In 3D this would lead to prohibitively long calculation times of well over a few months. Therefore, a 2D model was preferred, and the geometry is illustrated in Figure 5. Two packing beads are on top of each other in the discharge gap, which connects the grounded electrode with the dielectric material that covers the powered electrode. The contact points between the beads and the walls are slightly enlarged to overcome computational difficulties. In the first instance, the model used He as the discharge gas because we wanted to elucidate the electric field enhancement, which will be roughly independent of the gas used, and the reaction set of this
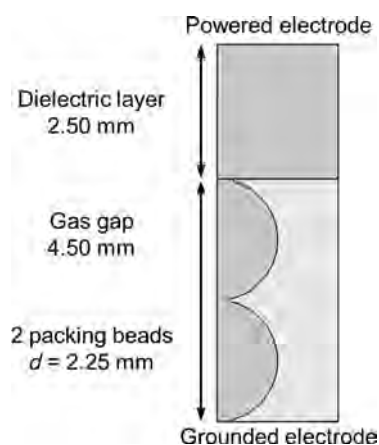

Figure 4. Scheme of the experimental setup. HV indicates the high voltage source

Figure 5. Geometry of the axisymmetric 2D model with two packing beads on top of each other in the gas gap.

noble gas is much simpler than that for CO_2, which thus limited the calculation time. Moreover, He is able to form a homogeneous instead of a filamentary discharge, which was simulated with the fluid model. The model considered six different species, that is, electrons (e), neutral helium atoms (He), positive helium ions (He$^+$), positive helium molecular ions (He$_2$$^+$), metastable helium atoms He(2^1S) and He(2^3S) combined into one effective level (He*), and helium dimers (He$_2$*). The different species interact with each other by 23 different reactions (Table 1).

The reaction rate coefficients of the electron impact reactions (R1–R5) are calculated as a function of the mean electron energy by using Bolsig+,[26] a software program that solves the Boltzmann equation for electrons using the input collision cross-sections, which are adopted here from the LXcat database.[26,27]

It also calculates the electron transport coefficients as a function of the mean electron energy. The reaction rate coefficients of the other 18 reactions, which are mainly recombination reactions with electrons and heavy particle reactions between ions, atoms, and excited species, are taken from literature.[28,29] Typically, the expressions are a function of the electron temperature and sometimes also of the gas temperature. However, the latter was kept constant at 300 K in our model. On top of this reaction set, four surface reactions are included, namely, the quenching of atomic and molecular metastables (i.e., He* and He2*) and recombination of the ions (i.e., He$^+$ and He$_2$$^+$) to ground-state helium atoms with a probability of 0.05 to emit a secondary electron of 5 eV.

The mobilities of the ions are taken from the literature,[30] namely, 1.0×10^{-3} m^{2}V^{-1}s^{-1} for He$^+$ and 1.6×10^{-3} m^{2}V^{-1}s^{-1} for He$_2$$^+$, and were used in the Einstein relationship to calculate the corresponding diffusion coefficients to yield values of 2.6×10^{-3} and 4.1×10^{-3} m^{2}s^{-1}, respectively. For the neutral species, the Chapman–Enskog equation was used to calculate the diffusion coefficients, which led to 1.68×10^{-4} m^{2}s^{-1} for He and He* and 1.45×10^{-4} m^{2}s^{-1} for He$_2$*.

The development of the 2D model was very challenging, and will be described in detail in a future paper. It should be stressed that this model only serves here to help explain the experimental observations and not to reproduce the experiments, which is beyond the current possibilities of the model.

Acknowledgements

Keywords: carbon dioxide · computational chemistry · energy conversion · plasma chemistry · sustainable chemistry

Table 1. Helium reaction set with rate coefficient equations.

No.	Reaction	Rate coefficient[a]	Ref.
R1	e+He→He+e	cross-section	[27]
R2	e+He→He*+e	cross-section	[27]
R3	e+He*→He+e	cross-section	[26]
R4	e+He→He$^+$+2e	cross-section	[27]
R5	e+He*→He$^+$+2e	cross-section	[27]
R6	e+He$_2$*→2He+e	3.8×10^{-15}	[28], [29]
R7	2e+He$^+$→He*+e	6.0×10^{-20} $(T_e/T_g)^{-4.4}$	[29]
R8	2e+He$_2$$^+$→He*+He+e	4.0×10^{-20} $(T_e/T_g)^{-1}$	[29]
R9	e+He$_2$$^+$+He→He*+2He	5.0×10^{-27} $(T_e/T_g)^{-1}$	[29]
R10	2e+He$_2$$^+$→He$_2$*+e	4.0×10^{-20} $(T_e/T_g)^{-1}$	[29]
R11	e+He$_2$$^+$+He→He$_2$*+He	5.0×10^{-27} $(T_e/T_g)^{-1}$	[29]
R12	e+He$_2$*→He$_2$$^+$+2e	9.75×10^{-10} $T_e^{0.71}$ e$^{-3.4/T_e}$	[29]
R13	e+He$^+$+He→He*+He	1.0×10^{-26} $(T_e/T_g)^{-2}$	[29]
R14	e+He$_2$$^+$→He$_2$*	5.0×10^{-9} $(T_e/T_g)^{-1}$	[29]
R15	He*+He*→He$_2$$^+$+e	2.03×10^{-9} $(T_g/0.025)^{0.5}$	[29]
R16	He*+He*→He$^+$+He+e	8.7×10^{-10} $(T_g/0.025)^{0.5}$	[29]
R17	He$^+$+2He→He$_2$$^+$+He	1.4×10^{-31} $(T_g/0.025)^{-0.6}$	[29]
R18	He*+2He→He$_2$*+He	8.1×10^{-36} T_g' e$^{-650/T_g'}$	[29]
R19	He$_2$*+He*→He$^+$+2He+e	2.03×10^{-9} $(T_g/0.025)^{0.5}$	[29]
R20	He$_2$*+He*→He$_2$$^+$+He+e	8.7×10^{-10} $(T_g/0.025)^{0.5}$	[29]
R21	He$_2$*+He$_2$*→He$^+$+3He+e	2.03×10^{-9} $(T_g/0.025)^{0.5}$	[29]
R22	He$_2$*+He$_2$*→He$_2$$^+$+2He+e	8.7×10^{-10} $(T_g/0.025)^{0.5}$	[29]
R23	He$_2$*+He→3He	4.9×10^{-22}	[28]

[a] T_e is the electron temperature [eV], T_g the gas temperature [eV], and T_g' the gas temperature [K]; the rate coefficients are in units of cm^{3}s^{-1} for two-body reactions and in cm^{6}s^{-1} for the three-body reactions.

[1] M. Aresta, *Carbon Dioxide as a Chemical Feedstock*, Wiley-VCH, Weinheim, **2010**.

[2] M. M. Halmann, M. Steinberg, *Greenhouse Gas Carbon Dioxide Mitigation: Science and Technology*, CRC Press, Boca Raton, **1999**.

[3] Z. Jiang, T. Xiao, V. L. Kuznetsov, P. P. Edwards, *Philos. Trans. R. Soc. London Ser. A* **2010**, *368*, 3343–3364.

[4] U. Kogelschatz, B. Eliasson, W. Egli, *J. Phys. IV* **1997**, *7*, 47–66.

[5] U. Kogelschatz, *Plasma Chem. Plasma Process.* **2003**, *23*, 1–46.

[6] A. P. H. Goede, W. A. Bongers, M. F. Graswinckel, R. M. C. M. van de Sanden, M. Leins, J. Kopecki, A. Schulz, M. Walker, *EPJ Web Conf.* **2014**, *79*, 01005.

[7] R. Aerts, W. Somers, A. Bogaerts, *ChemSusChem* **2015**, *8*, 702–716.

[8] H. L. Chen, H. M. Lee, S. H. Chen, M. B. Chang, *Ind. Eng. Chem. Res.* **2008**, *47*, 2122–2130.

[9] T. Nozaki, N. Muto, S. Kado, K. Okazaki, *Catal. Today* **2004**, *89*, 57–65.

[10] C.-L. Chang, T.-S. Lin, *Plasma Chem. Plasma Process.* **2005**, *25*, 227–243.

[11] H.-X. Ding, A.-M. Zhu, X.-F. Yang, C.-H. Li, Y. Xu, *J. Phys. D* **2005**, *38*, 4160–4167.

[12] K. Takaki, S. Takahashi, S. Mukaigawa, T. Fujiwara, K. Sugawara, T. Sugawara, *I. J. PEST*, **2009**, *3*, 28–34.

[13] A. Ogata, H. Einaga, H. Kabashima, S. Futamura, S. Kushiyama, H.-H. Kim, *Appl. Catal. B* **2003**, *46*, 87–95.

[14] X. Tu, H. J. Gallon, M. V. Twigg, P. A. Gorry, J. C. Whitehead, *J. Phys. D* **2011**, *44*, 274007.

[15] Q. Yu, M. Kong, T. Liu, J. Fei, X. Zheng, *Plasma Chem. Plasma Process.* **2012**, *32*, 153–163.

[16] D. Mei, X. Zhu, Y. He, J. D. Yan, X. Tu, *Plasma Sources Sci. Technol.* **2015**, *24*, 015011.

[17] J.-S. Chang, K. G. Kostov, K. Urashima, T. Yamamoto, Y. Okayasu, T. Kato, T. Iwaizumi, K. Yoshimura, *IEEE Trans. Ind. Appl.* **2000**, *36*, 1251.

[18] K. Takaki, J.-S. Chang, K. G. Kostov, *IEEE Trans. Dielectr. Electr. Insul.* **2004**, *11*, 481–490.

[19] W. S. Kang, J. M. Park, Y. Kim, S. H. Hong, *IEEE Trans. Plasma Sci.* **2003**, *31*, 504–510.

[20] H. Russ, M. Neiger, J. E. Lang, *IEEE Trans. Plasma Sci.* **1999**, *27*, 38.

[21] Q. Ye, T. Zhang, F. Lu, J. Li, Z. He, F. Lin, *J. Phys. D* **2008**, *41*, 025207.

[22] A. Fridman, *Plasma Chemistry*, CUP, New York, **2008**.

[23] L. F. Spencer, A. D. Gallimore, *Plasma Sources Sci. Technol.* **2013**, *22*, 015019.

[24] T. Nunnally, K. Gutsol, A. Rabinovich, A. Fridman, A. Gutsol, A. Kemoun, *J. Phys. D* **2011**, *44*, 274009.

[25] *Comsol*, http://www.comsol.com.

[26] G. J. M. Hagelaar, L. C. Pitchford, *Plasma Sources Sci. Technol.* **2005**, *14*, 722–733.

[27] Morgan database, www.lxcat.net, accessed 25 July **2013**.

[28] T. Martens, *Numerical Simulations of Dielectric Barrier Discharges*, PhD Thesis, University of Antwerp, **2012**.

[29] Q. Wang, D. J. Economou, V. M. Donnelly, *J. Appl. Phys.* **2006**, *100*, 023301.

[30] P. L. Patterson, *Phys. Rev. A* **1970**, *2*, 1154.